Stress–modulated remodelling of a non–homogeneous body

D. Ambrosi, A. Guillou,
Dipartimento di Matematica, Politecnico di Torino,
corso Duca degli Abruzzi 24, 10129 Torino, Italy.

E.S. Di Martino,
Institute for Complex Engineered Systems, Cardiovascular Biomechanics Lab,
Carnegie Mellon University, 5000 Forbes Ave, Pittsburgh, PA 15213, USA.

December 19, 2006

Abstract

Many soft tissues, and arteries *in primis*, exhibit residual stress after unloading, a characteristic related to the ability to self–organize their own constituents (cells and extracellular matrix proteins). This behavior can be theoretically predicted in a continuum mechanics framework assuming that the body self–remodels toward a *homeostatic* stress state. Open questions concern the characteristics of a stationary grown state, as dictated by the mechanical properties of the material and by the specific external load. In this paper we illustrate a mathematical framework and we perform numerical simulations for the remodelling of a two dimensional (axisymmetric) nonlinear elastic cylinder. In particular, we address the stress–modulated remodelling of the cylinder wall when local variations in the mechanical properties of the material occur. Our main result is that, as in one spatial dimension, the tendency of the system to homeostasis generates, thanks to the remodelling process, a residual stress that homogenizes the tension in the body under load. Possible physiological implications of this result are discussed in the final section.

Introduction

When observed on a sufficiently long time scale, biological systems are always open systems: they exchange mass and energy with the external environment. This characteristic makes the mathematical analysis of biological systems inherently more complex than that of purely mechanical ones, for which an assumption of a closed system is possible. The mechanics of soft tissues is a specific example of problems that must include external actions (e.g. nutrients and mass inflow) when considered on a time scale longer than a few days. The arterial wall mechanics, among this class of problems, is particularly interesting for two reasons. On one hand, its clinical interest is self-evident. On the other hand, in spite of numerous experimental works on the topic, the inner mechanisms of growth and residual stress creation are not yet well understood.

A related specific aspect of the complexity of biological systems is that their relationship with the surrounding environment forces them into a continuous evolutionary process so as to attain a steady state, generally known as homeostasis. Derived from the Greek (similar)

+ (to stand), homeostasis denotes the natural tendency of a living organism to maintain equilibrium. In order to maintain homeostasis, biological tissues undergo changes in mass as well as structural and functional adaptation to their environment. The present work focuses specifically on how the mechanical environment influences living tissues and, in particular, the category of biological tissues called soft tissues, which are characterized by large elastic deformations under typical physiologic loads. A basic hypothesis used in the present model is that the gradual remodelling of soft biological tissues, through growth or resorption of cells and extracellular components, is directly linked to the stress within the tissue and that remodelling proceeds toward stress homeostasis.

Despite the long-standing literature on the subject, a proper mathematical framework to describe the volumetric growth of an elastic continuum body has been formulated only quite recently. The seminal paper in this respect is due to Rodriguez et al. [25], who first introduced the decoupling of the tensor gradient of deformation into two multiplicative contributions: one accounting for growth and the other describing the mechanical behavior resulting from the relaxed (grown) configuration. This key idea has provided a correct kinematic framework within which it is now possible to account for volumetric growth in soft tissues and their elastic response from a stress-free state, in which possible residual stresses also vanish. The evolution of the growth tensor (or, in other words, the evolution of the local stress-free reference configuration) calls for a supplementary constitutive relation that drives the mass increment/reduction in the body.

The mathematical literature dealing with growth mechanics is quite recent. One question regards stability and has been recently investigated by Ben Ammar and Goriely [5]. They analyze the stability of a grown neo-Hookean incompressible spherical shell under external pressure. The importance of residual stress is established by showing that under large anisotropic growth a spherical shell can become spontaneously unstable without any external loading.

Another key point is the definition of a growth law of a the soft tissue, the *growth dynamics*. In general, this will depend on many chemo-mechanical factors, including the availability of nutrients. To date, few heuristic laws for understanding growth based on experimental observations have been devised, and they are in essence based on the theory of homeostatic stress. The most relevant contribution is due to Taber and Eggers [30], who assume that the growth of an artery, schematically represented by a homogeneous elastic annulus of Fung-like material, is ruled by the achievement of a radially constant equilibrium circumferential stress (the Cauchy one) and that this drives the system toward the associated residual tensional state.

Thermodynamically admissible growth laws have been devised in the mixture framework, where mass production is duly represented as phase exchange between components [13, 19]. In a one–component framework, one analysis of the admissible growth laws on the basis of thermodynamic arguments is due to DiCarlo and Quiligotti [8]. They state an a priori dissipative principle, involving standard forces and *accretive* forces, that has to be satisfied for any growth process. The exploitation of this inequality yields constitutive relationships that provide a direct coupling between stress and growth in terms of an Eshelby-like tensor. This approach has been further investigated by Ambrosi and Guana [1], who show that suitable assumptions on the general model lead back to the one proposed by Taber and Eggers as a small strain limit.

Numerical experiments prove the effectiveness of growth laws under one–dimensional (radially symmetric) assumptions. In the specific case of non–homogeneous mechanical prop-

erties, purely radial growth has been considered by Taber and Humphrey [31]; their model reproduces the dependence of the circumferential stress of an annulus on the radial coordinate.

The aim of our study was to investigate, by numerical simulation, the role of the remodelling process in a non-homogeneous axisymmetric thick-walled cylinder, mimicking an aortic vessel under some geometrical simplifications. The mathematical model was proposed by Ambrosi and Guana in [1]; here the equations are extended to a 2D axisymmetric geometry. The vessel wall is made of non-linear orthotropic hyperelastic material. The wall is supposed to be stiffer in some part, an assumption that recalls the typical changes observed in an abdominal aortic aneurysm [14] and intracranial fusiform aneurysms [27], and is in agreement with the observed regional stiffening of the aorta with age [32]. The system evolves towards a homeostatic state, assumed to be independent of possible local variations in the elastic properties. The results of the numerical simulations elucidate the role of stress homeostasis in more than one dimension, as will be discussed in the final remarks.

1 General theory of growth

Residual stress is a fundamental feature in the study of soft biological tissues such as arteries. Its existence in blood vessels has been revealed by Fung [12] via a simple experiment in which an unloaded arterial ring is cut along the radial direction and subsequently opens up, relieving internal stresses. For some time, the configuration generated by a radial cut of this type, namely the *opened-up* configuration, was thought to be a very good approximation of the stress-free state of an artery, since subsequent radial cuts did not reveal the presence of significant additional residual stresses. However, a few years later, Vossoughi et al. [33] provided us with an additional insightful experiment in which arteries were cut along the midline of the open sector which had been obtained by a previous radial cut. They found the inner segment to open further, while the outer one closed considerably. This experimental result unveiled the fact that the opened-up configuration was not entirely free of stresses and that a proper approximation of the geometry of the stress–free state in an arterial ring, may be more difficult to obtain than it had been initially thought. In fact, nowadays, it is often assumed that such a stress–free configuration for arteries might be unreachable in reality, as it has proven impossible to release all residual stresses within an arterial soft tissue.
The overall distribution of residual stresses throughout an arterial wall may be, very generally, described as follows. First, as noted by Fung [12], residual stresses cannot be uniformly distributed across the wall. Moreover, the residual circumferential stresses are known to be compressive in the inner part of the arterial wall, while tensile in the outer part (see, for example, [12] or [16]). At this point, one might reasonably ask what is the purpose of residual stresses in arteries. A possible explanation for their existence as been postulated by [12]. As observed by Fung, the circumferential stress distribution of a hypothetical residual stress–free vessel would experience, in normal working conditions, a high stress gradient near the inner boundary of the vessel. Biologically, this implies that without the presence of residual stress the blood vessel would be less resistent to changes in loads. By contrast, once residual stresses were included in the calculation of the circumferential stress *in vivo*, circumferential stress was found to be almost uniform throughout the arterial wall. Finally, let us note that, residual stresses are generated in the artery by non–uniform growth and remodelling, as noted by Skalak et al. [28]. Furthermore, the uniformity of the circumferential stress *in vivo* will prove crucial herein, as it is one of the main concept on which the growth law used in the

present analysis was based.

Kinematics

Let us consider a body which, at an initial time t_0, is in the stress-free configuration $\mathcal{B}_0$. A material point in this configuration is characterized by its coordinates $\mathbf{X}$. The body is subsequently subjected to some external loads and is assumed to encounter volumetric growth. At a time t, the loaded grown body occupies the region $\mathcal{B}_t$, in which a material point is represented by the position vector $\mathbf{x}$. The deformation from $\mathcal{B}_0$ to $\mathcal{B}_t$ is characterized by a one-to-one mapping, denoted by $\boldsymbol{\chi}$, such that $\mathbf{x} = \boldsymbol{\chi}(\mathbf{X}, t)$ for all $\mathbf{X}$ in $\mathcal{B}_0$, and the deformation gradient from $\mathcal{B}_0$ to $\mathcal{B}_t$ is then defined by $\mathbf{F} = \partial\mathbf{x}/\partial\mathbf{X}$. Following [25], we assume that the deformation gradient $\mathbf{F}$ may be theoretically decomposed into a growth part, represented by a so-called growth stretch tensor $\mathbf{G}$, and an elastic part, represented by an elastic tensor $\mathbf{F}_r$ (see Figure 1). The growth stretch tensor $\mathbf{G}$ can be thought of as characterizing the addition or removal of material at a point and the orientation of its deposition. In other words, $\mathbf{G}$ models the change in the local stress-free state of the body due to the growth and the grown stress-free configuration at time t is denoted by $\mathcal{B}_r$. The elastic tensor $\mathbf{F}_r$, ensures the continuity of the body as a whole by potentially giving rise to internal stresses, since growth is not, in general, geometrically compatible. The dashed line of Figure 1 points out that, in general, $\mathcal{B}_r$ is not a possible real configuration of the body; a complete stress relaxation is not possible, not even by breaking the body into a finite number of pieces. Let us note that $\mathbf{F}_r$ also contains information about the applied loads. The multiplicative decomposition of the total deformation gradient provides the relation $\mathbf{F} = \mathbf{F}_r\mathbf{G}$.

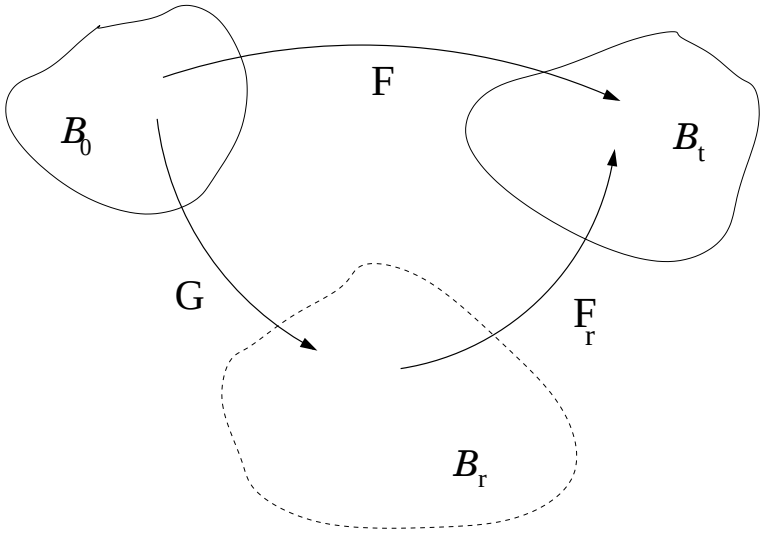

Figure 1: Schematic representation of the multiplicative decomposition of the tensor gradient of deformation $\mathbf{F} = \mathbf{F}_r\mathbf{G}$. $\mathcal{B}_0$ is the initial stress-free state, while $\mathcal{B}_r$ and $\mathcal{B}_t$ are, respectively, the grown stress-free state and loaded grown state of the body at time t (modified from [25]).

Dynamics

Since the aim of the present work was to model the mechanical behavior of the aortic wall, we assume the body to be made of nonlinear, hyperelastic, incompressible and non-homogeneous material. The active mechanical response of the material out of the grown stress-free configuration $\mathcal{B}_r$ is represented by a strain-energy function referred to as $\psi = \psi(\mathbf{F}_r, \mathbf{X})$. Note that, in the following, the aortic wall will be assumed as being piecewise homogeneous and the dependence of the strain energy on the reference position $\mathbf{X}$ will be relaxed for notational simplicity.
The incompressibility constraint yields $\det \mathbf{F}_r = 1$ and thus we have

$$\det \mathbf{F} = \det \mathbf{G} := J. \tag{1.1}$$

The Gateaux derivative of the strain energy is the stress tensor in the stress-free (grown) configuration $\mathcal{B}_r$. The standard Piola tensor of the active forces in $\mathcal{B}_t$ relative to the initial stress-free configuration $\mathcal{B}_0$ is denoted by $\mathbf{P}$ and is defined as $\mathbf{P} = J\mathbf{T}\mathbf{F}^{-T}$, where $\mathbf{T}$ is the Cauchy stress tensor in $\mathcal{B}_t$.
Since the growth tensor $\mathbf{G}$ is not, in general, the gradient of a deformation, no global change of coordinates exists between $\mathcal{B}_0$ and $\mathcal{B}_r$ and no differential form for the balance equations can be stated in $\mathcal{B}_r$. However, a local stress balance exists in $\mathcal{B}_r$ and tangent vectors can be pulled back from $\mathcal{B}_r$ to $\mathcal{B}_0$, where compatibility allows differential equations to be written. By exploiting multiplicative decomposition, together with the fact that the Cauchy stress is independent of the choice of a reference configuration, we obtain a relation for the active part of the Piola tensor $\hat{\mathbf{P}}$, namely

$$\hat{\mathbf{P}} = J \frac{\partial \psi}{\partial \mathbf{F}_r} \mathbf{G}^{-T}. \tag{1.2}$$

Moreover, the soft tissue is assumed to be incompressible and the stress tensor must therefore include a pressure term in order to accommodate such a constraint, i.e.

$$\mathbf{P} = J \frac{\partial \psi}{\partial \mathbf{F}_r} \mathbf{G}^{-T} - Jp\, \mathbf{F}_r^{-T} \mathbf{G}^{-T}, \tag{1.3}$$

and the Cauchy stress is given by

$$\mathbf{T} = \frac{\partial \psi}{\partial \mathbf{F}_r} \mathbf{F}_r^T - p\, \mathbf{I}. \tag{1.4}$$

In addition, the Piola tensor $\mathbf{P}$ in $\mathcal{B}_t$ relative to $\mathcal{B}_0$ must satisfy, in the absence of body forces, the equilibrium equation

$$\operatorname{Div} \mathbf{P} = \mathbf{0}. \tag{1.5}$$

Growth rate

Subsequent to the multiplicative decomposition of the total deformation gradient tensor, the standard balance of forces (1.5) must be supplemented by a new equation, which accounts for the time evolution of the growth tensor. In this paper we assumed that the growth tensor evolves according to the equation proposed by Ambrosi and Guana on the basis of thermodynamical arguments [1, 8], namely

$$\dot{\mathbf{G}} = -\mathrm{K}\,(\mathbb{E} - \mathbb{E}_0)\,\mathbf{G}, \tag{1.6}$$

where $\mathbb{E} = \mathbf{F}_r^T \mathbf{T} \mathbf{F}_r^{-T} - \psi \mathbf{I}$ is the Eshelby tensor, while K and $\mathbb{E}_0$ are, in the simplest case, constant matrices. The quantity $\mathbb{E}_0$ represents the homeostatic value of the Eshelby tensor, *i.e.* the equilibrium value in the system of ordinary differential equations (1.6). It is worth observing that, in general, the matrix multiplication of the relationship (1.6) intrinsically relates *every* component of the growth tensor to *every* component of the stress tensor. The decoupled growth law proposed by Taber and Eggers [30] can be recovered from the growth law (1.6) in the limit of small deformations. The Eshelby tensor as a tensorial function of the stress is duly frame–indifferent (it does not change for rotations of the reference frame), while its linearized counterpart, the Cauchy stress, does not.

The introduction of equation (1.6) in the theory can be accepted not only if suitable thermodynamic inequalities are satisfied, but also if the parameters involved in the equation can be identified by independent measures. In the specific case of Equation (1.6), how can one measure $\mathbb{E}_0$? At this stage, it is worth recalling a particular feature that arterial tissues *in vivo* are known to exhibit. Biologically, the homeostatic state of an artery refers to the state of equilibrium encountered by a young healthy mature artery *in vivo* and is generally associated with a so-called homeostatic pressure. Among other researchers, Liu and Fung [20] [21] experimentally noticed that the circumferential stress throughout the wall of an artery in this particular state is, in fact, uniform. This uniform circumferential stress is thus often referred to as the *homeostatic stress*. Moreover, the growth generated by a rise of the internal pressure in rat arteries has been obsevred to be accompanied by a return of the circumferential stress to a uniform value, so that, at the end of the growth, the mean hoop stress was nearly the same as that before the growth. Furthermore, Humphrey [16] recently pointed out that arterial growth is accompanied by the return of the axial stress near a uniform homeostatic value. These experimental results unveiled the fact that, in arteries, growth happens in parallel with the return of the circumferential and axial stresses to homeostatic levels. These important findings became a basis for the creation of a large amount of stress-related growth models for arteries (see Taber [29] or Rachev et al. [24], for example), and were also used in the present study. In other words, in the following, the equilibrium value $\mathbb{E}_0$ of the Eshelby tensor mentioned above will be explicitly related to the state of the circumferential and axial stresses in the homeostatic state, which therefore dictate the pattern of the growth.

2 Constitutive assumptions and geometrical modeling

The arterial wall response relative to $\mathcal{B}_r$ is assumed to obey the exponential strain energy constitutive equation proposed by Fung [11]

$$\psi = \frac{C}{2} \exp\left(a_1 E_{rr}^2 + a_2 E_{zz}^2 + a_3 E_{\theta\theta}^2 + a_4 E_{rz}^2 + a_5 E_{r\theta}^2 + a_6 E_{z\theta}^2\right), \tag{2.1}$$

where C, $a_1, ..., a_6$ are material parameters, $\mathbf{E} = \frac{1}{2}\left(\mathbf{F}_r^T \mathbf{F}_r - \mathbf{I}\right)$ corresponds to the Green strain tensor and $\mathbf{I}$ represents the identity tensor.

The aorta, which is assumed to be made of non-homogeneous material, undergoes axis-symmetric displacement only. That is, the displacement vector, denoted by $\mathbf{u}$, is postulated to have the form $\mathbf{u} = (u_r, u_z, 0)$. Moreover, all the fields involved in the analysis are independent on the circumferential coordinate (i.e. $\partial/\partial\Theta = 0$ for any field).

On one hand, the displacement gradient, which is defined by $\mathbf{H} := \operatorname{Grad} \mathbf{u}$, is related to the total deformation gradient through the formula $\mathbf{F} = \mathbf{H} + \mathbf{I}$, and has the following components

in cylindrical coordinates

$$\mathsf{H} = \left[\begin{array}{ccc} \frac{\partial u_r}{\partial R} & \frac{\partial u_r}{\partial Z} & 0 \\ \frac{\partial u_z}{\partial R} & \frac{\partial u_z}{\partial Z} & 0 \\ 0 & 0 & \frac{u_r}{R} \end{array} \right]_{(r,z,\theta)} \tag{2.2}$$

On the other hand, we assume the growth stretch tensor $\mathbf{G}$ to be of diagonal form in cylindrical coordinates, i.e. we write $\mathsf{G} = \mathrm{diag}(g_r, g_z, g_\theta)$. This simplification could be further extended to the case of a spherical form for the growth tensor: $\mathbf{G} = g\mathbf{I}$. However, we retain the possibility that growth occurs at different rates along different directions, since biological observations suggest that arteries grow, in general, in a non–uniform manner. For example, it is now well established that, in response to a persistent hypertensive pressure, an artery will grow in thickness, while encountering no change in its lumen radius, if its internal blood flow remains unchanged. By contrast, an increase in the internal blood flow of an artery, with no change in its internal pressure, is known to generate an increase in the artery internal radius, while preserving its thickness (see [22], for example). Let us note briefly that an explanation for these experimental results lies in the internal organization, at the cellular level, of the arterial wall. That is, on one hand, the organization of smooth muscle cells, for example, within an artery is such that they are disposed along the circumferential or axial directions. On the other hand, at maturity, cells are known to grow primarily through hypertrophic processes (i.e. cell enlargement), either by encountering changes in their diameter or changes in their length. Thus, non–uniform growth seems to prevail in arteries, with radial growth occurring as cells grow in diameters, a phenomenon that might be linked to possible changes in the internal pressure of an artery. If cells encounter growth in their length, the artery is then subject to circumferential or axial growth, a process that seems to be linked to hypothetical changes in blood flow. In order to provide expressions for the components of the Green strain $\mathbf{E}$, in the chosen system of coordinates, the tensor $\mathbf{E}$ is rewritten in terms of the displacement gradient $\mathbf{H}$ and the growth stretch tensor $\mathbf{G}$, namely

$$\mathbf{E} = \frac{1}{2}\left(\mathbf{G}^{-T}(\mathbf{H}+\mathbf{I})^T(\mathbf{H}+\mathbf{I})\mathbf{G}^{-1} - \mathbf{I}\right). \tag{2.3}$$

Thus, after some basic calculations, which are detailed in the separate Appendix, the components of the Green strain may be expressed as

$$\begin{cases} E_{rr} = \frac{1}{2g_r^2}\left[\left(\frac{\partial u_r}{\partial R}+1\right)^2 + \left(\frac{\partial u_z}{\partial R}\right)^2 - g_r^2\right], \\ E_{zz} = \frac{1}{2g_z^2}\left[\left(\frac{\partial u_z}{\partial Z}+1\right)^2 + \left(\frac{\partial u_r}{\partial Z}\right)^2 - g_z^2\right], \\ E_{\theta\theta} = \frac{1}{2g_\theta^2}\left[\left(\frac{u_r}{R}+1\right)^2 - g_\theta^2\right], \\ E_{rz} = E_{zr} = \frac{1}{2g_r g_z}\left[\frac{\partial u_r}{\partial Z}\left(\frac{\partial u_r}{\partial R}+1\right) + \frac{\partial u_z}{\partial R}\left(\frac{\partial u_z}{\partial Z}+1\right)\right], \\ E_{r\theta} = E_{\theta z} = E_{z\theta} = E_{\theta z} = 0. \end{cases} \tag{2.4}$$

Finally, by using equations (2.4) and (2.1) in (1.3), expressions for the components of the Piola stress may be found (see relations (A.12)).

In the cylindrical system of coordinates considered here, and when the symmetries involved in the problem are taken into account, the equilibrium equations (1.5) generates two non-

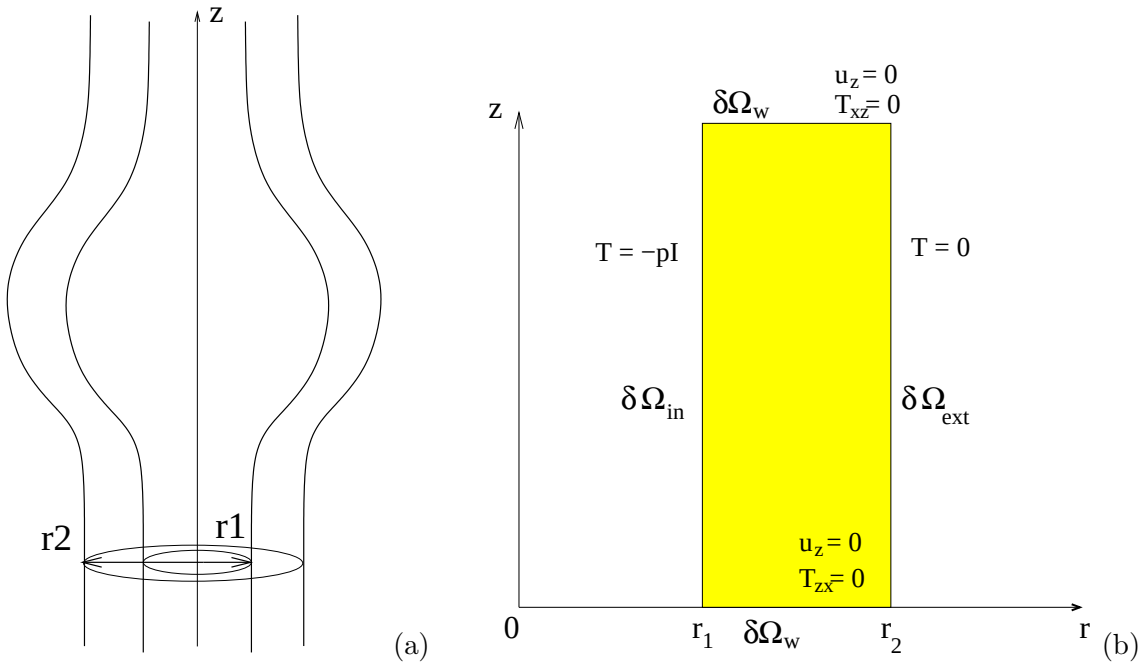

Figure 2: Sketch of the physical problem (a) and two–dimensional computational domain (b) in a material (Lagrangian) frame of reference. The conditions imposed at the boundaries are shown.

trivially solved equations, one in the radial direction and one in the axial direction:

$$\frac{\partial P_{rr}}{\partial R} + \frac{\partial P_{zr}}{\partial Z} + \frac{P_{rr} - P_{\theta\theta}}{R} = 0, \tag{2.5}$$

$$\frac{\partial P_{rz}}{\partial R} + \frac{P_{rz}}{R} + \frac{\partial P_{zz}}{\partial Z} = 0. \tag{2.6}$$

This system is subject to the boundary conditions

$$\begin{aligned} \mathbf{PN} &= \sqrt{\mathbf{N}\cdot\mathbf{C}^{-1}\mathbf{N}}\,\boldsymbol{\tau}, && \text{on } \partial\Omega_{in}, \\ \mathbf{PN} &= 0, && \text{on } \partial\Omega_{ext}, \\ \mathbf{PN}\cdot\mathbf{N}^{\perp} = 0, \mathbf{u}\cdot\mathbf{N} &= 0, && \text{on } \partial\Omega_{w}, \end{aligned}$$

where $\mathbf{C} := \mathbf{F}^T\mathbf{F}$ is the right Cauchy-Green tensor, while $\mathbf{N}$ and $\mathbf{N}^{\perp}$ are, respectively, the normal and tangential unit vectors to the boundary of the body in the stress-free state $\mathcal{B}_0$. The tension $\boldsymbol{\tau}$ accounts for the load at the internal wall due to the blood fluid. In general $\boldsymbol{\tau}$ includes normal and shear stresses. However, in the numerical simulations illustrated in the next section, we restrict our attention to the case of null shear stress. Let us note also that the external wall $\partial\Omega_{ext}$ is free of loads. Furthermore, the aortic specimen is supposed to displace freely in the radial direction and is subject to a null displacement condition along the z–axis on the boundary $\partial\Omega_w$.
Moreover, let us recall that the force balance equations are to be supplemented by the incompressibility constraint

$$\det \mathbf{F}_r = 1. \tag{2.7}$$

Finally, the material and geometrical parameters used in the present work are taken from values obtained for the rat aorta [31] (in non–dimensional form)

$$\begin{aligned} C =& 400 \qquad (a_1, a_2, a_3, a_4, a_5, a_6) = (0.01, 0.09, 0.17, .01, 0.001, 0.02)\,, \\ R_1 =& 0.8, \qquad R_2 = 1, \qquad \mathbb{E}_{0,\theta\theta} = -5 \qquad \mathbb{E}_{0,zz} = -1. \end{aligned}$$

The applied load at the internal wall is a pure pressure corresponding to 8 kPa.

3 Numerical simulation

3.1 Biomedical motivations

One possible application of the present study is to provide a proper 2D numerical framework to simulate the evolution of a axisymmetric fusiform aneurysm in the aorta. It is therefore worth mentioning briefly some relevant works dealing with mathematical modelling of aneurysmal tissues.

Aneurysms and, in particular, abdominal aortic aneurysms (AAA) are thought to form as a result of degradation of the Elastin (probably initially due to an injury in the tissue) and, more specifically, of degradation of the elastin laminae, as observed by Anidjar et al. [3]. As mentioned by Humphrey [15], the fact that the abdominal aorta is exposed to a large pulse pressure and the presence of bifurcations nearby (which induce additional pressure waves in the blood flow), may partly explain why this specific location seems to be a preferential site for aneurysms formation. Furthermore, an important observation, which motivates the present study, is that the overall mechanical properties of aneurysmal tissue differ from the properties of healthy arterial tissues. That is, AAA have been reported to be less extensible and stiffer than control ones (see He and Roach [14], for example). The observed stiffening of the aortic tissue appears to pre-exist the formation of an aneurysm, as demonstrated by Vande Geest et al. [32], who showed that the aortic tissue mechanical properties change from a high extensibility for young tissue to a much stiffer response and lower areal strain for older tissue. Interestingly the study also found that the abdominal section of the aorta appears to stiffen first, temporally, than the thoracic segments of the aorta. A closer look at the histology of aneurysmal tissue may partly explain the changes observed in the macroscopic mechanical behavior of this particular diseased tissue. In fact, the proportion of elastin and smooth muscle cells in AAA is dramatically lowered and the remaining elastin is, in general, fragmented and damaged. In contrast, the proportion of collagen and ground matrix increases considerably, which might explain the increase in stiffness encountered with this type of lesion. Although collagen is often held responsible for the strength of healthy arterial tissue, it is worth emphasizing that the collagen in the lesion is usually disorganized and not fully cross linked (see Freestone et al. [10]), making the wall weaker, although stiffer, in the presence of an aneurysm.

Most theoretical frameworks under which aneurysmal tissues are studied are based on the nonlinear theory of elastic membranes, such as in the work of Elger et al. [9] and Sacks et al. [26]. Although their work provides good insights on the mechanical behaviour of aneurysms, membrane theories implies to approximate the aneurysm as a thin-walled structure. In the present work, we consider the aneurysm to be thick-walled, thereby enabling the non-negligible effects of residual stresses in the tissue to be accounted for. Let us note briefly that another

excellent recent work on aneurysms, which deserves to be mentioned here, is the one by Baek et al. [4], in which they presented a constraint mixture theory framework for the study of thin-walled intracranial fusiform aneurysms.

3.2 Methods

In the numerical simulations the growth tensor is supposed to be of diagonal form and, in addition, we assume that only circumferential and axial growth occurs, i.e. $\mathbf{G} = \mathrm{diag}\,(1, g_z, g_\theta)$. The adoption of the multiplicative decomposition of the deformation tensor in an orthotropic nonlinear elasticity framework using a material frame of reference gives rise to quite a complex form for the final equations, as illustrated in the Appendix. Even more relevant is the high nonlinearity of the components of the Piola tensor (A.12).
The equations are discretized in time by a backward Euler finite difference discretization. The solution, evaluated at a time $t = n\Delta t$, is denoted by (u_r^n, u_z^n, p^n, g^n), so that, at every time step, the linearized components of the Piola stress tensor can be expressed as

$$\begin{cases} P_{rr}^{n+1} = g^n\, a_1 \left[\frac{\partial u_r^n}{\partial R}\frac{\partial u_r^{n+1}}{\partial R} + 2\frac{\partial u_r^{n+1}}{\partial R} + \frac{\partial u_z^n}{\partial R}\frac{\partial u_z^{n+1}}{\partial R}\right]\psi^n - p^{n+1}\,\frac{g^n}{K^n}\left(1 + \frac{u_r^n}{R} + \frac{\partial u_z^n}{\partial Z} + \frac{u_r^n}{R}\frac{\partial u_z^n}{\partial Z}\right), \\ P_{zz}^{n+1} = g^n\, a_2 \left[\frac{\partial u_z^n}{\partial Z}\frac{\partial u_z^{n+1}}{\partial Z} + 2\frac{\partial u_z^{n+1}}{\partial Z} + \frac{\partial u_r^n}{\partial Z}\frac{\partial u_r^{n+1}}{\partial Z}\right]\psi^n - p^{n+1}\,\frac{g^n}{K^n}\left(1 + \frac{u_r^n}{R} + \frac{\partial u_r^n}{\partial R} + \frac{u_r^n}{R}\frac{\partial u_r^n}{\partial R}\right), \\ P_{\theta\theta}^{n+1} = \frac{1}{(g^n)^2}\, a_3 \left[\frac{u_r^n}{R}\frac{u_r^{n+1}}{R} + 2\frac{u_r^{n+1}}{R} + 1 - (g^n)^2\right]\psi^n - p^{n+1}\, g^n \left(\frac{R}{R+u_r^n}\right), \\ P_{rz}^{n+1} = g^n\, a_4 \left[\frac{\partial u_r^{n+1}}{\partial Z}\left(\frac{\partial u_r^n}{\partial R} + 1\right) + \frac{\partial u_z^{n+1}}{\partial R}\left(\frac{\partial u_z^n}{\partial Z} + 1\right)\right]\psi^n + p^{n+1}\,\frac{g^n}{K^n}\,\frac{\partial u_z^n}{\partial R}\,(1 + \frac{u_r^n}{R}), \\ P_{zr}^{n+1} = g^n\, a_4 \left[\frac{\partial u_r^{n+1}}{\partial Z}\left(\frac{\partial u_r^n}{\partial R} + 1\right) + \frac{\partial u_z^{n+1}}{\partial R}\left(\frac{\partial u_z^n}{\partial Z} + 1\right)\right]\psi^n + p^{n+1}\,\frac{g^n}{K^n}\,\frac{\partial u_r^n}{\partial Z}\,(1 + \frac{u_r^n}{R}), \end{cases} \tag{3.1}$$

where $K^n = \left(1 + \frac{u_r^n}{R}\right)\left(1 + \frac{\partial u_r^n}{\partial R} + \frac{\partial u_z^n}{\partial Z} + \frac{\partial u_r^n}{\partial R}\frac{\partial u_z^n}{\partial Z} - \frac{\partial u_r^n}{\partial Z}\frac{\partial u_z^n}{\partial R}\right)$ and $\psi^n = \psi(u_r^n, u_z^n, g^n)$.
We observe that the incompressibility constraint (2.7) can be expanded in terms of $\mathbf{H}_r$ as

$$\begin{aligned} 1 =& \det(\mathbf{F}_r) = \det(\mathbf{I} + \mathbf{H}_r) = 1 + \mathrm{trace}(\mathbf{H}_r) + o(||\mathbf{H}_r||), \\ =& 1 + \frac{1}{g_r}\frac{\partial u_r}{\partial R} + \frac{1}{g_z}\frac{\partial u_z}{\partial Z} + \frac{1}{g_\theta}\frac{u_r}{R} + o(||\mathbf{H}_r||). \end{aligned} \tag{3.2}$$

In the present context, we restrict our attention to the incompressibility constraint being numerically satisfied to first order in $\mathbf{H}_r$, thus requiring that

$$\frac{1}{g_r^n}\frac{\partial u_r^{n+1}}{\partial R} + \frac{1}{g_z^n}\frac{\partial u_z^{n+1}}{\partial Z} + \frac{1}{g_\theta^n}\frac{u_r^{n+1}}{R} = 0. \tag{3.3}$$

The constraint (3.3) makes the global problem a saddle point one to the solution for the force balance equation (2.5)-(2.6). All fields are here represented by linear finite elements on a triangular unstructured mesh, thus requiring a suitable stabilization method that we implement by a penalty approach [6]. Standard details on finite element implementation are omitted. We just note that, thanks to the weak formulation, no further derivation of the nonlinear components of the Piola stress (3.1) has to be carried out. The resulting linear system is solved by a BI-CGSTAB solver.

3.3 Results

The numerical results illustrated in the present section are represented in a system of coordinates fixed in space ($\mathcal{B}_t$ of Figure 1) and the stress components refer to the Cauchy stress tensor (1.4).

Let us first consider a vessel with homogeneous mechanical properties. In such a case, axial displacement vanishes too, and the solution does not depend on the axial coordinate. We therefore recover the one-dimensional (radial) solutions, already discussed in several past articles [1, 30].

Figure 3(a) illustrates the hoop stress field in the loaded cylinder in its steady state after the remodelling process. The peak values differ significantly from the ones obtained in the same body before the reorganization machinery starts up (not shown; ranging between 23.4 and 34.8). The radial plot of the residual stress (Figure 3(b)) reproduces qualitatively the behavior theoretically predicted by Ogden [23] and this test is actually used as an indirect way to fix the value of the parameters $\mathbb{E}_{0,\theta\theta}$ and $\mathbb{E}_{0,zz}$.

Following [31], material inhomogeneity is introduced in the cylinder supposing that the wall is twice stiffer in the middle region ($C = 800$) than in the upper and lower ones ($C = 400$). Note that, as mentioned in the introduction, the present choice of a stiffer region for modelling the lesion is motivated by experimental observations made on aneurysmal tissues, such as the ones by He and Roach [14], as well as by the observation by Vande Geest et a. [32]. The coefficient varies linearly between these two values in narrow transition layers (width equal to 0.1) centered in 0.65 and 0.35.

Figure 4(b) shows the map of the determinant of $\mathbf{G}$, after remodelling, in the inhomogeneous loaded cylinder. Basically, this graph measures the mass addition/resorption that has been produced during the growth in order to achieve the final configuration. It is important to emphasize that the numerical values obtained here are not to be taken as absolute values. That is, one should keep in mind that the initial conditions are given in an abstract configuration and not in a real biological state, since, development of soft tissues and residual stress production occur contiguously *in vivo*, so that no intact stress–free artery can be observed in nature. The idea that lies behind this model, and which has been used in several existing growth models, is that residual stresses in mature vessels may be produced as a mean to reach a homeostatic stress state. In the present model, the homeostatic stress state is mathematically represented by a steady state solution of the system of equations (1.6), irrespective of the initial state. The values of the determinant of $\mathbf{G}$ detail here the pattern of mass re–organization that generates the residual stress.

Figures 4(a) and 5(a) show the hoop stress, in the non–homogeneous vessel, before and after remodelling, respectively. Despite its physiological irrelevance, *in se*, their comparison reveals essential characteristics of the remodelling process. Growth in the aorta mostly occurs in the stiffer region, as illustrated by the value of the determinant of the growth tensor (Figure 4(b)). The thickening of the stiffer part of the body causes the hoop stress field to be strongly smoothed by growth, as the range of values obtained for the hoop stress goes from (19,47.5) to (28.9,32.5). The tension in the softer region is very close to the values obtained in the homogeneous case presented in 3(a), The maximum value tension in the remodelled wall occurs in the transition layer between different values of C, while in the non–remodelled one it is maximum at the internal wall.

A more biologically noteworthy comparison can be obtained facing Figures 4(a) and 5(b). The latter plot represents the hoop stress field in the wall of a non–homogeneous axisym-

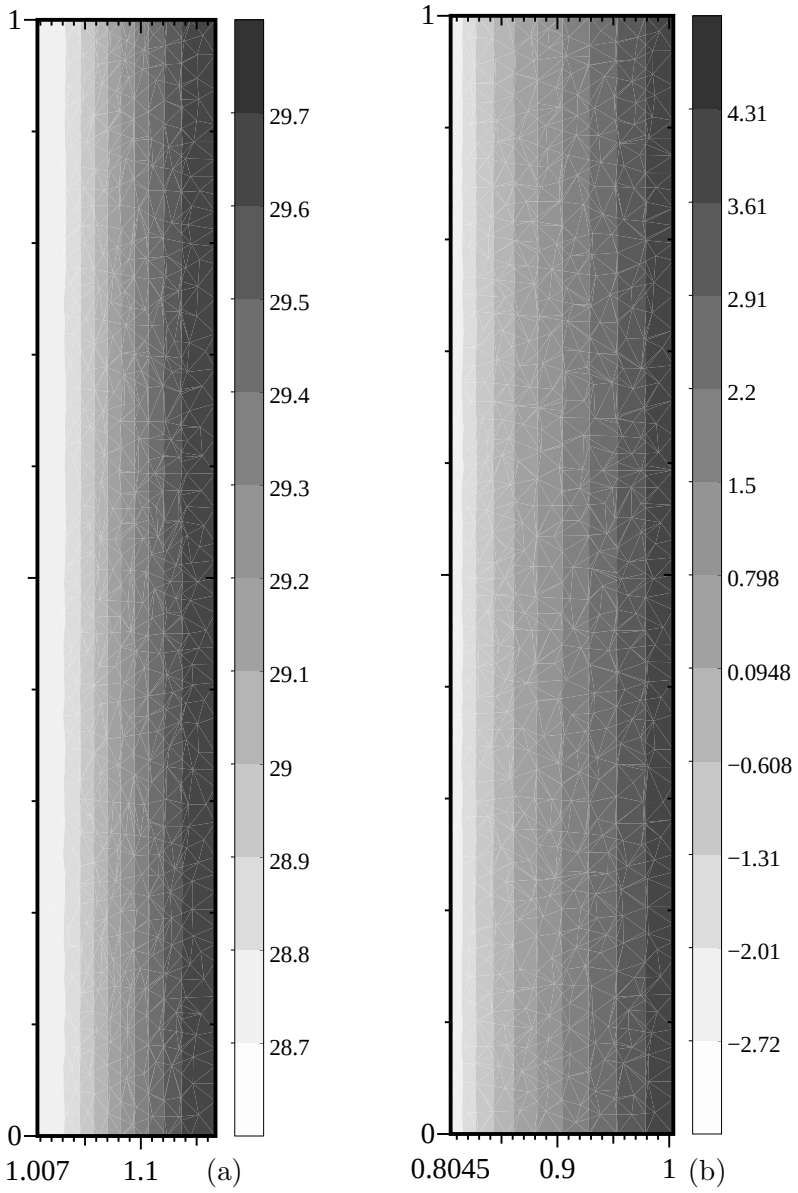

Figure 3: Hoop stress under load (a) and residual hoop stress (b) in a homogeneous axisymmetric cylinder, at the end of the remodelling process. The solution of this problem is independent of the z coordinate. The material organization in the loaded body homogenizes the stress inside a small interval $(28.7, 29.7)$. The behavior of the residual stress is dictated by the value of $\mathbb{E}_0$.

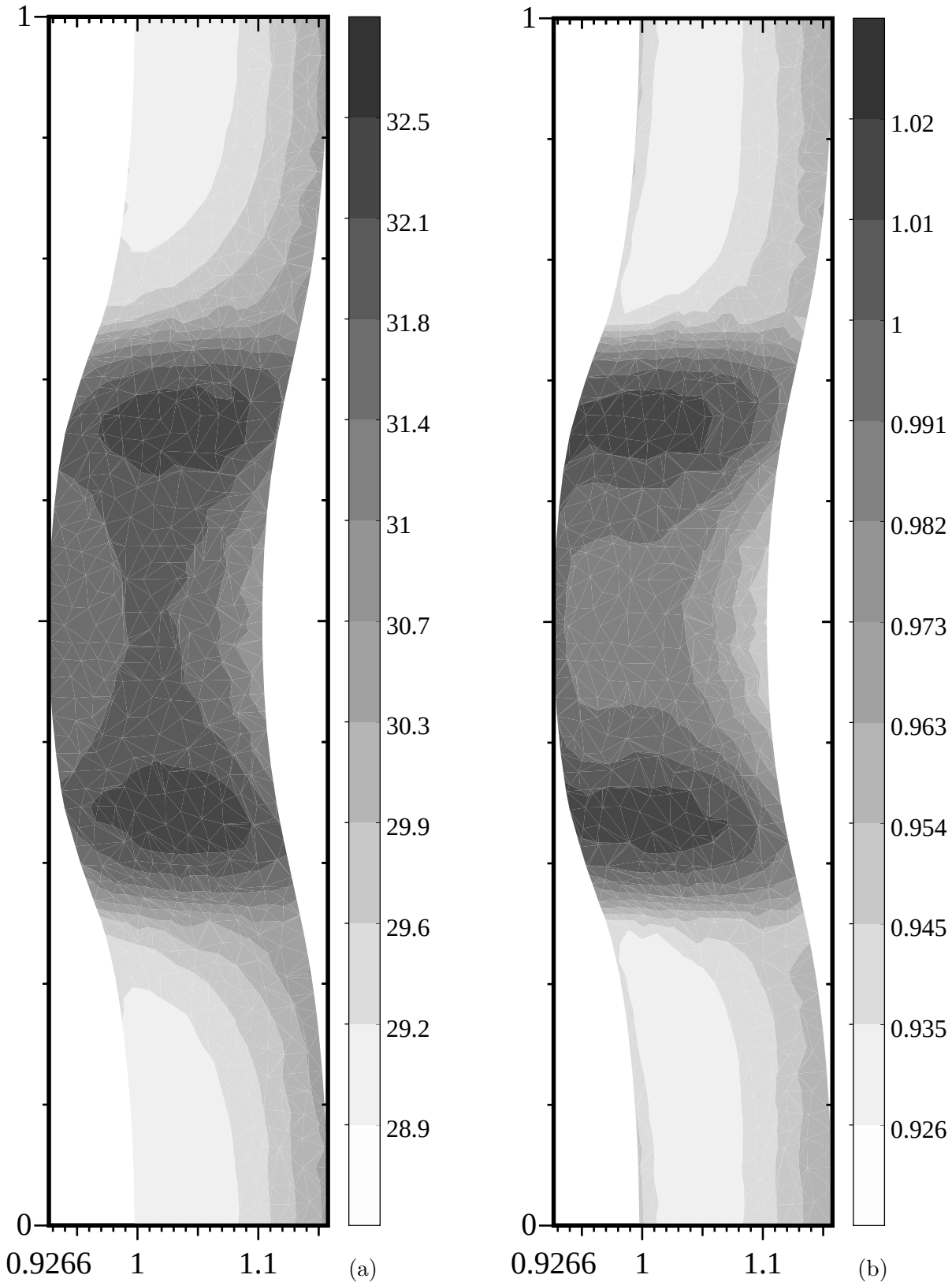

Figure 4: Hoop stress (a) and determinant of the growth tensor (b) in a non–homogeneous arterial wall after remodelling.

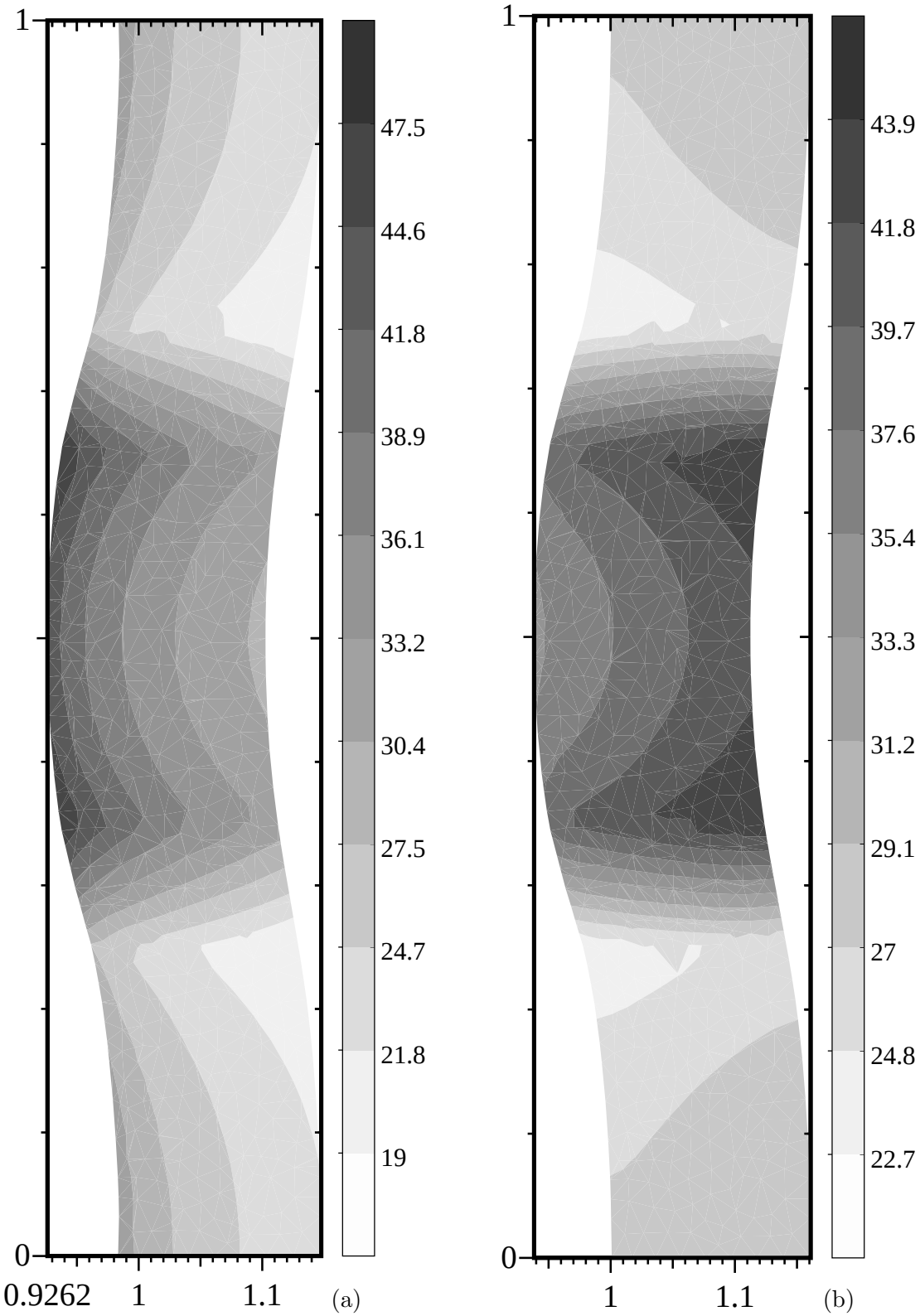

Figure 5: Hoop stress in a non–homogeneous arterial wall before remodelling (a) or after remodelling occurred on the basis of a homogeneous stress field (b), under load. Note that the greyscales of the two figures (and Figure 4(a)) are different.

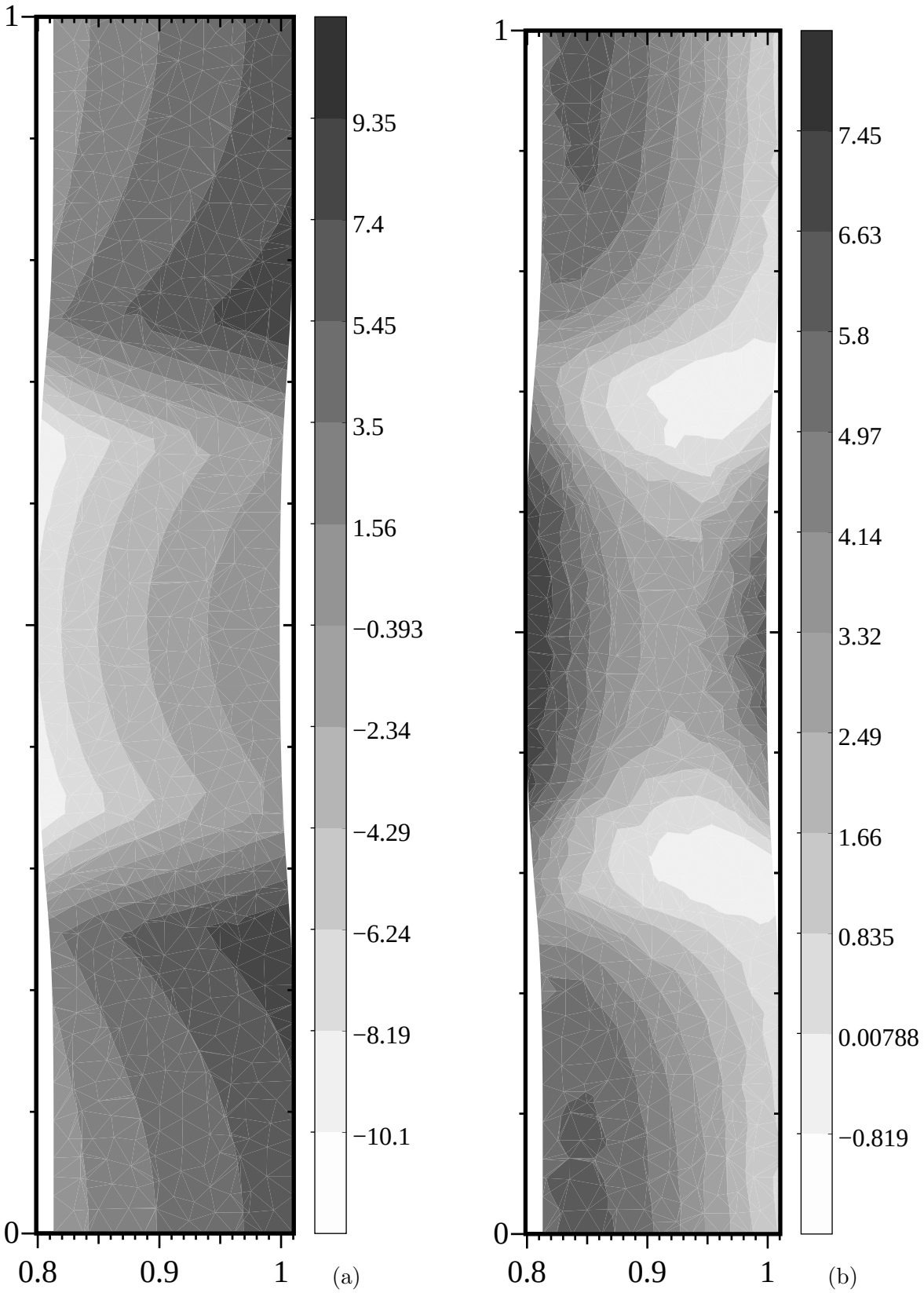

Figure 6: Residual hoop (a) and axial (b) stress field in a non–homogeneous arterial wall after remodelling.

metric cylinder that has previously undergone a remodelling process driven by homogeneous mechanical properties. In other words, it is the hoop stress in a body that first has grown in response to a given stress field like the ones of Figures 4 and then changes its mechanical characteristics in a time much shorter than the remodelling one. The stress range is here somewhat intermediate between the previous ones, with higher values on the external wall. The components of the residual stress in the unloaded body can be computed by solving the force balance equations after remodelling. Figures 5(a) and 5(b) reveal that, according to the present model, residual hoop stress in a non-homogeneous vessel can be locally compressive, which is in accordance with previous experimental observations (see [12], for example). The same remark, although less evident, holds for the form of the axial residual stress distribution: both tension and compression are locally observed but the integral value provides the expected tensional state. Note that boundary conditions along the z-axis prescribe null displacement only: in the present framework *all* residual stress in the body must arise from the remodelling process.

Final remarks

This paper discusses the results of two–dimensional numerical simulations for the mathematical modeling of volumetric growth in an elastic body. The equations of the system are the standard force balance supplemented by an equation coupling stress and growth; as a specific target, the equations are applied to a two–dimensional axisymmetric case with non–homogeneous mechanical characteristics.

The adopted growth–law is a simple example of constitutive equation satisfying a dissipation principle. The model is able to predict the formation of both hoop and axial residual stresses in the body, by stress–modulated growth.

The introduction of a multiplicative decomposition of the tensor gradient of deformation originates a number of algebraic complications. However, the calculations detailed in the Appendix show that the model is kept to a reasonable feasibility.

The illustrated mathematical model does not involve tunable parameters; in principle, any parameter appearing in the equations can be fixed on the basis of direct or indirect comparison with experiments. A direct measure can provide the parameters of the stress–strain relationship, while stress homogenization arguments can provide the homeostatic stress value $\mathbb{E}_0$ [23].

The numerical simulations suggest that the theory of stress–modulated remodelling can be an effective tool to study two dimensional (axisymmetric) problems. The results show that, at least in some range of parameters, when one considers a cylinder wall with local stiffening, the residual stress field homogenizes the stress around an average value dictated by homeostasis, which is the same behavior predicted in one dimension. We remark that this is not a self–evident statement, because stress and growth are here tensorial quantities and it is not clear a priori how the components are to be coupled. In this paper it was assumed that only two components of the growth tensor evolve, (g_z, g_θ), and their dynamics depend on the components of the strain tensor via the Eshelby tensor. Several other possibilities remain to be explored.

The content of this paper is mainly methodological. Some aspects of the model do not satisfy yet a full biomechanical applicability: the material is homogeneous and the boundary conditions do not correspond to a physiological pressure (16 KPa). The latter issue involves

questions of numerical stability that remain to be explored [18]. However the numerical simulations are carried out for a geometry, material properties, and loads that are close to the physiological conditions encountered by rat arteries. Questions about possible physiological relevance of the results naturally arise. The results obtained are preliminary and no quantitative prediction can be expected yet. However, the simulations corroborate the conjecture that a correct functioning of stress homeostasis should stabilize the vessel wall under local changes of the mechanical properties. A major disease of the artery is the formation of an aneurysm, which arises from degeneration of the artery's connective tissue. The aortic wall has been observed to become increasingly stiffer with age, and that the process is heterogeneous, starting earlier in the life of the patient for the abdominal portion of the aorta [32]. One may wonder if this observed change in material properties may elicit the formation of aneurysm. These early simulations suggest that, at least in the small range of parameters considered up to now, healthy homeostasis goes towards a re-equilibration of the vessel system and should not be accounted among the possible factors producing the growth of an aneurysm. On the other hand, if the stress–driven remodelling for some reason does not work properly, larger stresses can be produced. This kind of qualitative speculations goes in the same direction of the arguments provided by Humphrey and Canham [17], who discriminate among several possible mechanisms for the rupture of cerebral aneurysms and finally point the attention on the remodelling process. We believe that a framework like the one presented in this paper can provide useful advancements in this direction.

A Equations in cylindrical coordinates

The Green strain tensor can be written as

$$\mathbf{E} = \frac{1}{2}\left(\mathbf{F}_r^T\mathbf{F}_r - \mathbf{I}\right) = \frac{1}{2}\left(\mathbf{G}^{-T}\mathbf{F}^T\mathbf{F}\mathbf{G}^{-1} - \mathbf{I}\right) = \frac{1}{2}\left(\mathbf{G}^{-T}(\mathbf{H}+\mathbf{I})^T(\mathbf{H}+\mathbf{I})\mathbf{G}^{-1} - \mathbf{I}\right), \quad \text{(A.1)}$$

where $\mathbf{I}$ is the identity tensor, $\mathbf{G}$ corresponds to the growth stretch tensor and $\mathbf{H} = \operatorname{Grad}\mathbf{u}$ denotes the gradient of the displacement $\mathbf{u}$, which is assumed to have the form $\mathbf{u} = (u_r, u_z, 0)$. Moreover, in our problem, we considered no dependence on the coordinate Θ and the components of the tensors $\mathbf{G}$ and $\mathbf{H}$ in cylindrical coordinates are given by

$$\mathsf{G} = \operatorname{diag}(g_r, g_z, g_\theta), \quad \mathsf{H} = \begin{bmatrix} \frac{\partial u_r}{\partial R} & \frac{\partial u_r}{\partial Z} & 0 \\ \frac{\partial u_z}{\partial R} & \frac{\partial u_z}{\partial Z} & 0 \\ 0 & 0 & \frac{u_r}{R} \end{bmatrix}. \quad \text{(A.2)}$$

Let us add briefly that, throughout the whole appendix, cylindrical components are provided in the form (r, z, θ).
On one hand, we have

$$\begin{aligned} \mathsf{G}^{-T}(\mathsf{H}+\mathsf{I})^T &= \begin{bmatrix} 1/g_r & 0 & 0 \\ 0 & 1/g_z & 0 \\ 0 & 0 & 1/g_\theta \end{bmatrix} \begin{bmatrix} H_{rr}+1 & H_{zr} & 0 \\ H_{rz} & H_{zz}+1 & 0 \\ 0 & 0 & H_{\theta\theta}+1 \end{bmatrix}, \\ &= \begin{bmatrix} \frac{H_{rr}+1}{g_r} & \frac{H_{zr}}{g_r} & 0 \\ \frac{H_{rz}}{g_r} & \frac{H_{zz}+1}{g_z} & 0 \\ 0 & 0 & \frac{H_{\theta\theta}+1}{g_\theta} \end{bmatrix}. \end{aligned} \quad \text{(A.3)}$$

Similarly, on the other hand, we have

$$
\begin{aligned}
(\mathsf{H}+\mathsf{I})\mathsf{G}^{-1} &= \begin{bmatrix} H_{rr}+1 & H_{rz} & 0 \\ H_{zr} & H_{zz}+1 & 0 \\ 0 & 0 & H_{\theta\theta}+1 \end{bmatrix} \begin{bmatrix} 1/g_r & 0 & 0 \\ 0 & 1/g_z & 0 \\ 0 & 0 & 1/g_\theta \end{bmatrix}, \\
&= \begin{bmatrix} \frac{H_{rr}+1}{g_r} & \frac{H_{rz}}{g_r} & 0 \\ \frac{H_{zr}}{g_r} & \frac{H_{zz}+1}{g_z} & 0 \\ 0 & 0 & \frac{H_{\theta\theta}+1}{g_\theta} \end{bmatrix}. \qquad \text{(A.4)}
\end{aligned}
$$

So, we obtain

$$
\mathsf{G}^{-T}(\mathsf{H}+\mathsf{I})^T(\mathsf{H}+\mathsf{I})\mathsf{G}^{-1} \begin{bmatrix} \frac{(H_{rr}+1)^2+H_{zr}^2}{g_r^2} & \frac{H_{rz}(H_{rr}+1)+H_{zr}(H_{zz}+1)}{g_r g_z} & 0 \\ \frac{H_{rz}(H_{rr}+1)+H_{zr}(H_{zz}+1)}{g_r g_z} & \frac{(H_{zz}+1)^2+H_{rz}^2}{g_z^2} & 0 \\ 0 & 0 & \frac{(H_{\theta\theta}+1)^2}{g_\theta^2} \end{bmatrix}. \qquad \text{(A.5)}
$$

The use of equation (A.5) and equation $(A.2)_2$ in equation (A.1) therefore yields, for the problem considered, expressions for the components of the Green strain tensor in cylindrical coordinates, namely

$$
\begin{cases}
E_{rr} = \frac{1}{2g_r^2}\left[\left(\frac{\partial u_r}{\partial R}+1\right)^2 + \left(\frac{\partial u_z}{\partial R}\right)^2 - g_r^2\right], \\
E_{zz} = \frac{1}{2g_z^2}\left[\left(\frac{\partial u_z}{\partial Z}+1\right)^2 + \left(\frac{\partial u_r}{\partial Z}\right)^2 - g_z^2\right], \\
E_{\theta\theta} = \frac{1}{2g_\theta^2}\left[\left(\frac{u_r}{R}+1\right)^2 - g_\theta^2\right], \\
E_{rz} = E_{zr} = \frac{1}{2g_r g_z}\left[\frac{\partial u_r}{\partial Z}\left(\frac{\partial u_r}{\partial R}+1\right) + \frac{\partial u_z}{\partial R}\left(\frac{\partial u_z}{\partial Z}+1\right)\right], \\
E_{r\theta} = E_{\theta z} = E_{z\theta} = E_{\theta z} = 0.
\end{cases} \qquad \text{(A.6)}
$$

The strain-energy function used for modelling the response of the material out of the grown stress-free state $\mathcal{B}_r$ is of Fung exponential type, namely

$$
\psi = \frac{C}{2}\exp\left(a_1E_{rr}^2 + a_2E_{zz}^2 + a_3E_{\theta\theta}^2 + a_4E_{rz}^2 + a_5E_{r\theta}^2 + a_6E_{z\theta}^2\right), \qquad \text{(A.7)}
$$

with C, $a_1, ..., a_6$ denoting material parameters. The Piola stress, in the incompressible case, is provided by the relation

$$
\mathbf{P} = J\frac{\partial\psi(\mathbf{F}_r)}{\partial\mathbf{F}_r}\mathbf{G}^{-T} - Jp\mathbf{F}_r^{-T}\mathbf{G}^{-T}, \qquad \text{(A.8)}
$$

where p corresponds to a Lagrange multiplier associated with the incompressibility constraint. This can be rewritten as

$$
\mathbf{P} = J\frac{\partial\psi(\mathbf{F}_r)}{\partial\mathbf{F}_r}\mathbf{G}^{-T} - Jp\left(\mathbf{H}+\mathbf{I}\right)^{-T}. \qquad \text{(A.9)}
$$

The quantity $(\mathbf{H}+\mathbf{I})^{-T}$ has the following component, in cylindrical coordinates,

$$
(\mathsf{H}+\mathsf{I})^{-T} \begin{bmatrix} \frac{1+H_{\theta\theta}+H_{zz}+H_{\theta\theta}H_{zz}}{K} & \frac{-H_{zr}(1+H_{\theta\theta})}{K} & 0 \\ \frac{-H_{rz}(1+H_{\theta\theta})}{K} & \frac{1+H_{\theta\theta}+H_{rr}+H_{\theta\theta}H_{rr}}{K} & 0 \\ 0 & 0 & \frac{1}{1+H_{\theta\theta}} \end{bmatrix}, \qquad \text{(A.10)}
$$

where $K = (1 + H_{\theta\theta})(1 + H_{rr} + H_{zz} + H_{rr}H_{zz} - H_{rz}H_{zr})$. Thus the cylindrical components of the Piola stress $\mathbf{P}$ are written as

$$\begin{cases} P_{rr} = 2g_\theta g_z a_1 E_{rr}\psi - p\, g_r g_\theta g_z \left(\frac{1+H_{\theta\theta}+H_{zz}+H_{\theta\theta}H_{zz}}{K}\right), \\ P_{zz} = 2g_r g_\theta a_2 E_{zz}\psi - p\, g_r g_\theta g_z \left(\frac{1+H_{\theta\theta}+H_{rr}+H_{\theta\theta}H_{rr}}{K}\right), \\ P_{\theta\theta} = 2g_r g_z a_3 E_{\theta\theta}\psi - p\, g_r g_\theta g_z \left(\frac{1}{1+H_{\theta\theta}}\right), \\ P_{rz} = 2g_r g_\theta g_z a_4 E_{rz}\psi + p\, g_r g_\theta g_z \left(\frac{H_{zr}(1+H_{\theta\theta})}{K}\right), \\ P_{zr} = 2g_r g_\theta g_z a_4 E_{rz}\psi + p\, g_r g_\theta g_z \left(\frac{H_{rz}(1+H_{\theta\theta})}{K}\right), \\ P_{r\theta} = P_{\theta r} = P_{z\theta} = P_{\theta z} = 0. \end{cases} \tag{A.11}$$

By using equation (A.6), this may be rewritten as

$$\begin{cases} P_{rr} = \frac{g_\theta g_z}{g_r^2}\, a_1 \left[\left(\frac{\partial u_r}{\partial R}+1\right)^2 + \left(\frac{\partial u_z}{\partial R}\right)^2 - g_r^2\right]\psi - p\,\frac{g_r g_\theta g_z}{K}\left(1 + \frac{u_r}{R} + \frac{\partial u_z}{\partial Z} + \frac{u_r}{R}\frac{\partial u_z}{\partial Z}\right), \\ P_{zz} = \frac{g_r g_\theta}{g_z^2}\, a_2 \left[\left(\frac{\partial u_z}{\partial Z}+1\right)^2 + \left(\frac{\partial u_r}{\partial Z}\right)^2 - g_z^2\right]\psi - p\,\frac{g_r g_\theta g_z}{K}\left(1 + \frac{u_r}{R} + \frac{\partial u_r}{\partial R} + \frac{u_r}{R}\frac{\partial u_r}{\partial R}\right), \\ P_{\theta\theta} = \frac{g_r g_z}{g_\theta^2}\, a_3 \left[\left(\frac{u_r}{R}+1\right)^2 - g_\theta^2\right]\psi - p\, g_r g_\theta g_z \left(\frac{R}{R+u_r}\right), \\ P_{rz} = g_\theta\, a_4 \left[\frac{\partial u_r}{\partial Z}\left(\frac{\partial u_r}{\partial R}+1\right) + \frac{\partial u_z}{\partial R}\left(\frac{\partial u_z}{\partial Z}+1\right)\right]\psi + p\,\frac{g_r g_\theta g_z}{K}\,\frac{\partial u_z}{\partial R}\,(1+\frac{u_r}{R}), \\ P_{zr} = g_\theta\, a_4 \left[\frac{\partial u_r}{\partial Z}\left(\frac{\partial u_r}{\partial R}+1\right) + \frac{\partial u_z}{\partial R}\left(\frac{\partial u_z}{\partial Z}+1\right)\right]\psi + p\,\frac{g_r g_\theta g_z}{K}\,\frac{\partial u_r}{\partial Z}\,(1+\frac{u_r}{R}), \\ P_{r\theta} = P_{\theta r} = P_{z\theta} = P_{\theta z} = 0, \end{cases} \tag{A.12}$$

where $K = \left(1 + \frac{u_r}{R}\right)\left(1 + \frac{\partial u_r}{\partial R} + \frac{\partial u_z}{\partial Z} + \frac{\partial u_r}{\partial R}\frac{\partial u_z}{\partial Z} - \frac{\partial u_r}{\partial Z}\frac{\partial u_z}{\partial R}\right)$.

The equilibrium equations are given by the relation $\mathrm{Div}\,\mathbf{P} = 0$. In cylindrical coordinates, this provides equations in the radial, circumferential and axial directions, namely

$$0 = \frac{1}{R}\frac{\partial(RP_{rr})}{\partial R} + \frac{1}{R}\frac{\partial P_{\theta r}}{\partial \Theta} + \frac{\partial P_{zr}}{\partial Z} - \frac{P_{\theta\theta}}{R}, \tag{A.13}$$

$$0 = \frac{1}{R}\frac{\partial(RP_{rz})}{\partial R} + \frac{1}{R}\frac{\partial P_{\theta z}}{\partial \Theta} + \frac{\partial P_{zz}}{\partial Z}, \tag{A.14}$$

$$0 = \frac{1}{R}\frac{\partial(RP_{r\theta})}{\partial R} + \frac{1}{R}\frac{\partial P_{\theta\theta}}{\partial \Theta} + \frac{\partial P_{z\theta}}{\partial Z} + \frac{P_{\theta r}}{R}. \tag{A.15}$$

The solution of the circumferential equation (A.15) is trivial, while the radial equation (A.13) and the axial equation (A.14) may be rewritten as

$$0 = \frac{1}{R}\frac{\partial(RP_{rr})}{\partial R} + \frac{\partial P_{zr}}{\partial Z} - \frac{P_{\theta\theta}}{R}, \tag{A.16}$$

$$0 = \frac{1}{R}\frac{\partial(RP_{rz})}{\partial R} + \frac{\partial P_{zz}}{\partial Z}, \tag{A.17}$$

where the specific forms for P_{rr}, P_{zr}, $P_{\theta\theta}$, P_{rz} and P_{zz} are provided by equation (A.12).

In addition, the Eshelby tensor is provided by the relation $\mathbb{E} = \mathbf{F}_r^T(\partial\psi/\partial\mathbf{F}_r) - \psi\mathbf{I}$. The components of the elastic tensor $\mathbf{F}_r$, in cylindrical coordinates, may be written as

$$\begin{aligned}\mathsf{F}_r^T = \mathsf{G}^{-T}\mathsf{F}^T = \mathsf{G}^{-T}(\mathsf{H}+\mathsf{I})^T &= \begin{bmatrix} 1/g_r & 0 & 0 \\ 0 & 1/g_z & 0 \\ 0 & 0 & 1/g_\theta \end{bmatrix} \begin{bmatrix} H_{rr}+1 & H_{zr} & 0 \\ H_{rz} & H_{zz}+1 & 0 \\ 0 & 0 & H_{\theta\theta}+1 \end{bmatrix}, \\ &= \begin{bmatrix} \frac{H_{rr}+1}{g_r} & \frac{H_{zr}}{g_r} & 0 \\ \frac{H_{rz}}{g_r} & \frac{H_{zz}+1}{g_z} & 0 \\ 0 & 0 & \frac{H_{\theta\theta}+1}{g_\theta} \end{bmatrix}, \end{aligned} \tag{A.18}$$

while the functional derivative $\partial\psi(\mathbf{F}_r)/\partial\mathbf{F}_r$, when written in terms of the Fung exponential strain energy function, takes the form

$$2\psi \begin{bmatrix} a_1E_{rr} & a_4E_{rz} & 0 \\ a_4E_{zr} & a_2E_{zz} & 0 \\ 0 & 0 & a_3E_{\theta\theta} \end{bmatrix}. \tag{A.19}$$

We therefore obtain

$$\mathsf{F}_r^T\frac{\partial\psi(\mathsf{F}_r)}{\partial\mathsf{F}_r} = 2\psi \begin{bmatrix} a_1E_{rr}\left(\frac{H_{rr}+1}{g_r}\right) + a_4\frac{E_{zr}H_{zr}}{g_r} & a_2\frac{E_{zz}H_{zr}}{g_r} + a_4E_{rz}\left(\frac{H_{rr}+1}{g_r}\right) & 0 \\ a_1\frac{E_{rr}H_{rz}}{g_r} + a_4E_{zr}\left(\frac{H_{zz}+1}{g_z}\right) & a_2E_{zz}\left(\frac{H_{zz}+1}{g_z}\right) + a_4\frac{E_{rz}H_{rz}}{g_r} & 0 \\ 0 & 0 & a_3E_{\theta\theta}\left(\frac{H_{\theta\theta}+1}{g_\theta}\right) \end{bmatrix}.$$

Finally, the cylindrical components of the Eshelby tensor may be expressed as

$$\begin{cases} \mathbb{E}_{rr} = \psi\left(2a_1E_{rr}\left(\frac{H_{rr}+1}{g_r}\right) + 2a_4\frac{E_{zr}H_{zr}}{g_r} - 1\right), \\ \mathbb{E}_{zz} = \psi\left(2a_2E_{zz}\left(\frac{H_{zz}+1}{g_z}\right) + 2a_4\frac{E_{rz}H_{rz}}{g_r} - 1\right), \\ \mathbb{E}_{\theta\theta} = \psi\left(2a_3E_{\theta\theta}\left(\frac{H_{\theta\theta}+1}{g_\theta}\right) - 1\right), \\ \mathbb{E}_{rz} = 2\psi\left(a_2\frac{E_{zz}H_{zr}}{g_r} + a_4E_{rz}\left(\frac{H_{rr}+1}{g_r}\right)\right), \\ \mathbb{E}_{zr} = 2\psi\left(a_1\frac{E_{rr}H_{rz}}{g_r} + a_4E_{zr}\left(\frac{H_{zz}+1}{g_z}\right)\right), \\ \mathbb{E}_{r\theta} = \mathbb{E}_{\theta r} = \mathbb{E}_{z\theta} = \mathbb{E}_{\theta z} = 0. \end{cases} \tag{A.20}$$

It is worth expressing as well the components of the Cauchy stress for the problem considered here. Recalling that, in the incompressible case, the Cauchy stress is given by $\mathbf{T} = (\partial\psi/\partial\mathbf{F}_r)\mathbf{F}_r^T - p\mathbf{I}$, the components of the Cauchy stress in cylindrical coordinates can

be written as

$$\begin{cases} T_{rr} = 2\psi \left(a_1 E_{rr} \left(\frac{H_{rr}+1}{g_r} \right) + a_4 \frac{E_{rz} H_{rz}}{g_r} \right) - p, \\ T_{zz} = 2\psi \left(a_2 E_{zz} \left(\frac{H_{zz}+1}{g_z} \right) + a_4 \frac{E_{zr} H_{zr}}{g_r} \right) - p, \\ T_{\theta\theta} = 2\psi \, a_3 E_{\theta\theta} \left(\frac{H_{\theta\theta}+1}{g_\theta} \right) - p, \\ T_{rz} = 2\psi \left(a_2 \frac{E_{zz} H_{rz}}{g_r} + a_4 E_{zr} \left(\frac{H_{rr}+1}{g_r} \right) \right), \\ T_{zr} = 2\psi \left(a_1 \frac{E_{rr} H_{zr}}{g_r} + a_4 E_{rz} \left(\frac{H_{zz}+1}{g_z} \right) \right), \\ T_{r\theta} = T_{\theta r} = T_{z\theta} = T_{\theta z} = 0. \end{cases} \tag{A.21}$$

Acknowledgments

This research has been partially supported by the FIRB 2001 Project "Metodi dell'Analisi Matematica in Biologia, Medicina e Ambiente".

References

[1] Ambrosi, D. and Guana, F., Stress–modulated growth, *Math. Mech. Solids*, to appear.

[2] Ambrosi, D. and Mollica, F., On the mechanics of tumor growth, *Int. J. Eng. Sci.*, **40**:1297–1316 (2002).

[3] Anidjar, S., Dobrin, P.B., Eichorst, M., Graham, G.P. and Chejfec, G. Correlation of inflammatory infiltrate with the enlargement of experimental aortic aneurysms. *J. Vasc. Surg.* **16**:139-147 (1992).

[4] Baek, S., Rajagopal, K.R. and Humphrey, J.D. A theoretical model of enlarging intracranial fusiform aneurysms. *J. Biomech. Eng.* **128**:142–149 (2006).

[5] Ben Amar M. and Goriely A., Growth and instabilities in elastic tissues, *J. Mech. Phys. Solids*, **53**:2284-2319 (2005).

[6] Bochev P.B. and Lehoucq R.B., Regularization and stabilization of discrete saddle-point variational problems, Electronic Transactions on Numerical Analysis, **22**:97-113 (2006).

[7] Chuong, C.J. and Fung, Y.C., On residual stresses in arteries. *J. Biomech. Eng.* **108**: 189–199 (1986).

[8] DiCarlo, A. and Quiligotti, S., Growth and balance, *Mech. Res. Commun.*, **29**:449–456 (2002).

[9] Elger, D., Blackketter, D., Budwig, R. and Johansen, K. The influence of shape on the stresses in model abdominal aortic aneurysms. *J. Biomech. Engr.* **118**:326-332 (1996).

[10] Freestone, T., Turner, R.J., Coady, A., Higman, D.J., Greenhalgh, R.M. and Powell, J.T. Inflammation and matrix metalloproteinases in the enlarging abdominal aortic aneurysm. *Arterioscler. Thromb. Vasc. Biol.* **15**:1145–1151 (1995).

[11] Fung, Y.C., Biomechanics, Springer-Verlag, New York, (1981).

[12] Fung, Y.C., Biodynamics: circulation, Springer-Verlag, New York, (1984).

[13] Fusi, L., Farina, A. and Ambrosi, D., Mathematical Modelling of a Solid–Liquid Mixture with Mass Exchange Between Constituents, *Math. Mech. Solids*, to appear.

[14] He, C. M. and Roach, M. R. The composition and mechanical properties of abdominal aortic aneurysms. *J. Vasc. Surg.* **20**:6–13 (1994).

[15] Humphrey, J.D. Mechanics of the arterial wall: review and directions. *Critical Review in Biomed. Engr.* **23(1/2)**:1–162 (1995).

[16] Humphrey, J.D., Continuum biomechanics of soft biological tissues, *Proceedings of the Royal Society*, **459**:3–46 (2003).

[17] Humphrey, J.D. and Canham, P.B., Structure, mechanical properties and mechanics of intercranial saccular aneurysms, *J. Elasticity*, **61**:49–81 (2000).

[18] Kuhl, E., Menzel, A. and Steinmann, P., Computational modeling of growth: A critical review, a classification of concepts and two new consistent approaches, *Comp. Mech.*, **32**:71-88 (2003).

[19] Loret, B. and Simões, M.F., A framework for deformation, generalized diffusion, mass transfer and growth in multi–species multi-phase biological tissues, *Eur. J. Mech A Solids*, **24** 757–781 (2005).

[20] Liu, S.Q. and Fung, Y.C., Relationship between hypertension, hypertrophy, and opening angle of zero-stress state of arteries following aortic constriction, *J. Biomech. Eng.* **111**:325–335 (1989).

[21] Liu, S.Q. and Fung, Y.C., Changes in the zero-stress state of rat pulmonary arteries in hypoxic hypertension, *J. Appl. Physiol.* **70**:2455–2470 (1991).

[22] Matsumoto, T. and Hayashi, K. (1994) Mechanical and dimensional adaptation of rat aorta to hypertension. *J. Biomech. Eng.* **116** 278–283.

[23] Ogden, R. W., Lecture Notes 6, Institute of Fundamental Technological Research, Polish Academy of Sciences, Warsaw *Nonlinear Elasticity with Application to Material Modelling*, (2003).

[24] Rachev, A., Stergiopulos, N. and Meister, J., A model for geometric and mechanical adaptation of arteries to sustained hypertension, *J. Biomech.* **120**:9–17 (1998).

[25] Rodriguez, E.K., Hoger, A. and McCulloch, A., Stress dependent finite growth in soft elastic tissues, *J. Biomechanics*, **27**:455–467 (1994).

[26] Sacks, M. S., Vorp, D. A., Raghavan, M. L., Federle, M. P. and Webster, M. W. In vivo three-dimensional surface geometry of abdominal aortic aneurysms. *Ann. Biomed. Engr.* **27**:469-480 (1999).

[27] Scott, S., Ferguson, G.G. and Roach, M.R., Comparison of the elastic properties of human intercranial arteries and aneurysms, *Can J. Physiol. Pharmacol.*, **50**:328–332 (1972).

[28] Skalak, R., Dasgupta, G., Moss, M., Otten, E., Dullemeijer, P. and Vilmann, H. Analytical description of growth. *J. Theor. Biol.*, **94**:555–577 (1982).

[29] Taber, L.A., A model for aortic growth based on fluid shear and fiber stresses, *J. Biomech. Eng.*, **120**:348–354 (1998).

[30] Taber, L. and Eggers, D.W., Theoretical study of stress modulated growth in the aorta, *J. Theor. Biol.* **180**:343–357 (1996).

[31] Taber, L. and Humphrey, J.D., Stress–modulated growth, residual stress and vascular heterogeneity, *ASME J. Biomech. Eng.* **123**:528–535 (2001).

[32] Vande Geest, J.P., Sacks, M.S. and Vorp D.A., Age dependency of the biaxial biomechanical behavior of human abdominal aorta, *J. Biomech. Eng.* **126**: 815-822 (2004).

[33] Vossoughi, J., Hedjazi, H. and Borris, F.S., Intimal residual stress and strain in large arteries, *ASME Bioengineering Conference*, Bed-Vol. **24**:434–437 (1993).